2016

Impact of a 12-volt Lead Acid Battery State-of-Charge on the Performance of an Automotive Air Conditioning System

Santanu Prasad Datta
Birla Institute of Technology & Science Pilani, Hyderabad Campus, India, spdatta@hyderabad.bits-pilani.ac.in

Prasanta Kumar Das
Indian Institute of Technology Kharagpur, 721302, India, pkd@mech.iitkgp.ernet.in

Siddhartha Mukhopadhyay
Indian Institute of Technology Kharagpur, 721302, India, smukh@ee.iitkgp.ernet.in

Impact of a 12-volt Lead Acid Battery State-of-Charge on the Performance of an Automotive Air Conditioning System

Santanu P. DATTA[*1], Prasanta K. DAS[2], Siddhartha MUKHOPADHYAY[3]

[1] Department of Mechanical Engineering
Birla Institute of Technology & Science Pilani– Hyderabad Campus, 500078, India
spdatta@hyderabad.bits-pilani.ac.in

[2] Department of Mechanical Engineering
Indian Institute of Technology Kharagpur, 721302, India
pkd@mech.iitkgp.ernet.in

[3] Department of Electrical Engineering
Indian Institute of Technology Kharagpur, 721302, India
smukh@ee.iitkgp.ernet.in

* Corresponding Author

ABSTRACT

In most of the Automotive Air Conditioning Systems (AACSs) though the compressor is powered by the car engine, the evaporator blower and the condenser fan are run by a 12-volt DC battery which is powered by an alternator. Any fault in the alternator, drops the battery output voltage. Owing to this, a stationary test rig for an AACS is developed with all actual automotive components. A continuous monitoring of the system performance is done at different battery charge level. It is observed that the evaporator blower and the condenser fan speed reduces continuously with the discharging of the storage battery, resulting a certain drop in air flow rate across the heat exchangers. Here, the continuous monitoring of the battery discharge voltage and its impact on the deterioration on the system cooling capacity, compression work, and the COP are reported.

1. INTRODUCTION

In traditional automobiles, run by combustion engines, auxiliary electric power is required by a variety of onboard functions ranging from cooling, lighting and crucial safety systems to car entertainment system. For example, in most of the Automotive Air Conditioning Systems (AACSs) though the compressor is directly powered by the car engine; the evaporator blower and the condenser fan are coupled to DC motors and require auxiliary DC power. In addition, the DC power is also used to invigorate the maneuvering of compressor clutch engagement and disengagement as well, and to empower a number of electronic switches, relays and sensors related to the AACS. Though the power requirement of many of the functions listed above are nominal, the evaporator blower and the condenser fan demands a continuous power supply. The storage battery can ensure the continuous supply of power as it replenishes the same from the car engine through a charging process. It is therefore needless to say that the battery voltage and its state-of-charge (SOC) is very important for the flawless onboard operation of several automotive systems including the AACS.

The lead acid battery which is a combination of lead plates and an electrolyte consisting of a diluted sulfuric acid, is an electrical storage device that convert electrical energy into potential chemical energy (Ceraolo, 2000). Capasso & Veneri (2014) experimentally analyzed the performance of two different lithium batteries ($Li[NiCoMn]O_2$ and $LiFePO_4$) with a lead acid battery from the point of view of their application as storage systems for road vehicles powered by an electric traction system. Interestingly, in charging state $Li[NiCoMn]O_2$ shows the high charging rate whereas, $LiFePO_4$ shows a better behavior during discharging state. Zhang et al. (2012) proposed a novel regulation system for a vehicle generator and lead acid battery system. By integrating the regulation method, the output voltage of the generator is determined and controlled by the algorithm to save electrical energy and protect the lead-acid battery.

Though there are number of literatures related to battery modeling and its application in electric or hybrid vehicles (Moseley, 1997; Omar et al., 2012; Veneri, Migliardini, Capasso, & Corbo, 2011), any such literature is not available on the effect of battery charge or discharge in its air conditioning system. However, few literature is available based on battery thermal management associated with environment temperature. Neubauer & Wood (2014) used Battery Lifetime Analysis and Simulation Tool for Vehicles (BLAST-V) to examine the sensitivity of Battery electric vehicles (BEV) utility to driver aggression and climate effects over the performance of the vehicle. They observed that in cold and hot climate the battery performance degrades due to inefficient cabin heating system and high peak on-road battery temperature accordingly. Xing et al. (2014) developed a temperature based battery model to estimate the effect of ambient temperature in between the relationship of open circuit voltage (OCV) and SOC.

The aim of this present work is to carry out an experimental analysis of the most commonly used lead acid battery as the sole power source for the prime movers of the AACS. A continuous monitoring of the battery charging and discharging process are observed. It is noted that the evaporator blower and the condenser fan speeds reduce continuously with the discharging of the storage battery, resulting a certain drop in air flow rate across the heat exchangers. Further, a detailed experimental study is conducted to evaluate the cooling capacity, compression work, and COP of the system with continuous discharging of the battery.

2. EXPERIMENTAL FACILITY AND TEST PROCEDURE

The performance of the lead acid battery is studied in a stationary test rig (Figure 1) of an automotive air conditioning system (AACS), developed for a four seater passenger car as described in (Datta et al., 2014; Datta et al., 2013). The test rig comprises a swash plate compressor, a condenser, an expansion valve, and an evaporator. Figure 2 describes the detail wire diagram of the AACS circuitry powered by the 12-volt lead acid battery with a capacity of 36Ah. The condenser fan and evaporator blower are driven by two separate DC motors energized by this battery source. At an optimum battery charge level, the condenser fan can operate at a constant speed (1750 rpm), whereas the blower could be operated at three different speeds of 2208, 3092 and 3475 rpm by varying the existing manual control switch set 1, set 2 and set 3. Further, the swash plate compressor does not run continuously but becomes operative as and when necessary through the operation of a magnetic clutch which is energized by the same battery source. The battery power is also necessary for the operation of the thermistor and the dual cut-off pressure switch. The thermistor is placed close to the evaporator surface towards the air outlet side to prevent frost formation in the evaporator. The dual pressure switch should also take care of the on-off cycle based on the pressure response at the compressor discharge side.

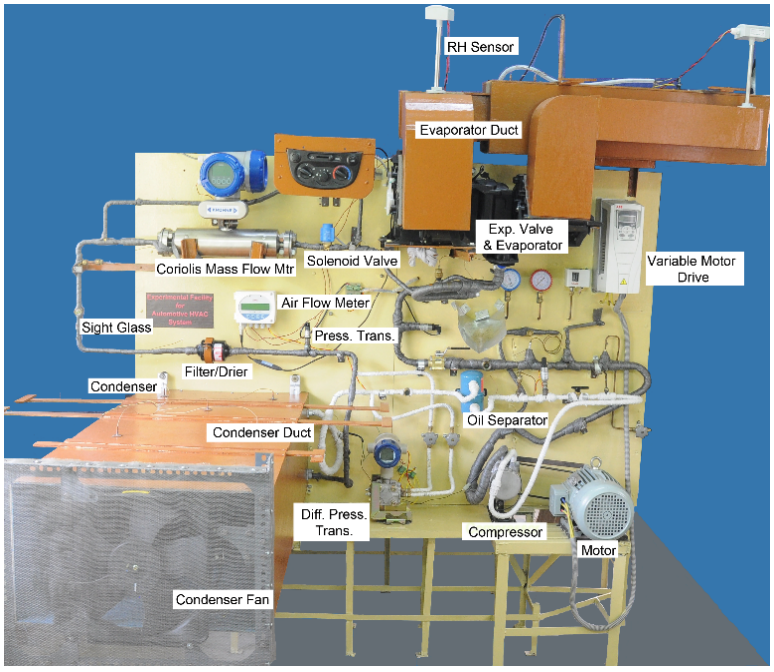

Figure 1: Photographic view of the test rig

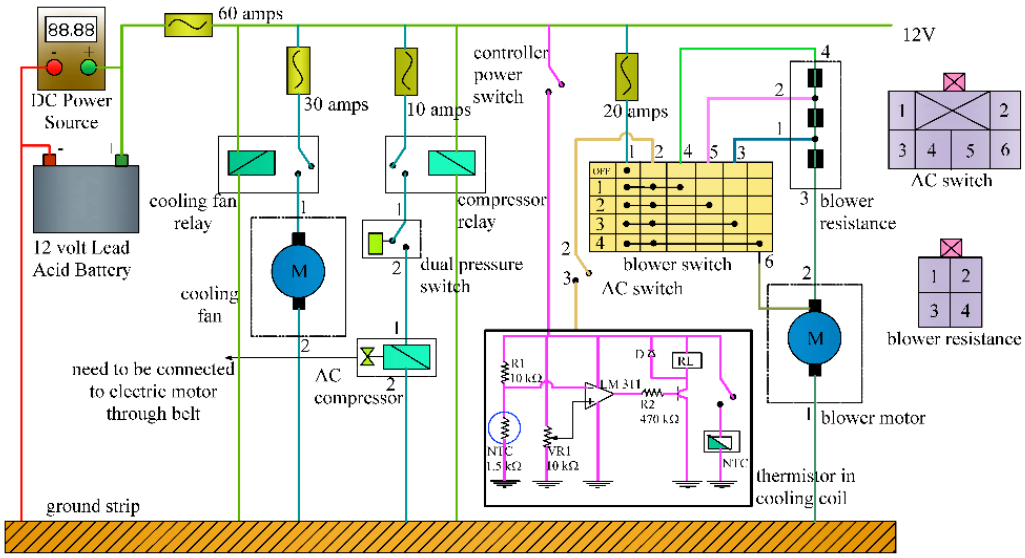

Figure 2: Electrical wire diagram of the AACS powered by 12V lead-acid battery

Experiments are planned to discharge the fully charged battery at a fixed compressor speed until the evaporator blower or the condenser fan stopped. It is observed that the compressor stops running ones the battery voltage drops down to 8 volts. However, the motors of the evaporator blower and the condenser fan are capable to run up to a much lower voltage of the battery. This gives an opportunity to investigate the performance of the battery along with the blower and the fan speed until the battery fully drainage. The experiments are conducted at 1200 rpm compressor speed with an average ambient temperature of 30 to 32ºC and a relative humidity of 70 to 80%. The battery characteristics along with the system performance are continuously monitored through a NI Data Acquisition System interfaced with LabVIEW (2010) platform.

3. DATA REDUCTION

3.1 Battery Performance

The rate of variation of battery terminal voltage is quantified as the battery state-of-charge (SOC), which can be defined as:

$$SOC = 100\left(1 - \frac{1}{C}\int_0^t i(t)dt\right) \tag{1}$$

where,

C = rated battery capacity (Ah)

$i_t = \int_0^t i(t)dt$ = actual battery capacity (Ah)

As per the manufacturers specifications the present battery has the capacity (C) of 36 Ah. One can experimentally estimate this capacity (C) with a vigorous number of tests. The battery capacity is a time variant and dependent upon the current profile. For most of the analysis it is assumed that the SOC for a fully charged battery is 100% at time, $t = 0$ whereas, it is 0% for an empty battery.

3.2 Automotive Air Conditioning Performance

The provision for temperature and pressure measurement at the inlet and exit of the compressor enables the estimation of enthalpy at these points. With the measured refrigerant mass flow rate, work done $\dot{W}_{comp}$ by the compressor can be estimated as follows:

$$\dot{W}_{comp} = \dot{m}_{comp}\left(h_{comp,out} - h_{comp,in}\right) \tag{2}$$

Where $h_{comp,out}$ and $h_{comp,in}$ are the enthalpies of the refrigerant at the inlet and outlet of the compressor respectively.
It may be noted that pressure measurement immediately before the evaporator is not possible due to shortage of space as the expansion valve and the evaporator make an integral part for the typical AACS components used to build the present set up. However, a reasonably good assessment of the pressure at the evaporator inlet can be made from the suction line pressure measurement which is almost constant throughout the line. Finally, the heat transfer of the evaporator or the cooling capacity $\left(\dot{Q}_{eva,ref}\right)$ can be obtained from the following relationship:

$$\dot{Q}_{eva,ref} = \dot{m}_{comp}\left(h_{eva,out} - h_{eva,in}\right) \tag{3}$$

where $h_{eva,out}$ and $h_{eva,in}$ are the enthalpies of the refrigerant at the inlet and outlet of the evaporator respectively.
Similarly, heat transfer through condenser $\left(\dot{Q}_{cond,ref}\right)$ can be obtained by estimating the enthalpy difference between the inlet and outlet conditions of the condenser as:

$$\dot{Q}_{cond,ref} = \dot{m}_{ref}\left(h_{cond,in} - h_{cond,out}\right) \tag{4}$$

Where $h_{cond,in}$ and $h_{cond,out}$ are the enthalpies of the refrigerant at the inlet and outlet of the condenser respectively.
It may be noted that condenser outlet refrigerant enthalpy cannot be determined precisely only through pressure and temperature measurements if the condensation is only partial. This generally happens when the system runs with less than adequate charge. In the present investigation we have not encountered such a situation.
Finally, the coefficient of performance (COP) of the system can be evaluated from experimental results from the refrigerant side as, the ratio of the cooling capacity to the compressor power.

$$COP_{ref} = \dot{Q}_{eva,ref} \Big/ \dot{W}_{comp} \tag{5}$$

4. RESULTS AND DISCUSSION

4.1 Charging Performance of the Lead Acid Battery

In the test rig, the charging of the battery takes place by using a DC power source with an initial current of 2.5 A. As the battery getting charged the current consumption also gradually decreases. The duration of the battery to get fully charged is around three hours. From Figure 3, it is observed that during this period, the voltage across the battery terminals increases in few steps to reach its maximum value whereas, the SOC (eq. 1) increases linearly. As the battery get fully charged, the SOC approaches to unity and remains constant even in overcharging. During the charging operation, a few steps in battery voltage is observed due to some chemical reactions inside the battery. Sulfuric acid with higher specific gravity is generated during the charging and sinks towards the bottom of the cell. As a result, the gradient in specific gravity produces an incorrect low reading at the top of the cell. Therefore, there is a certain voltage difference as indicated by the specific gravity at the top of the cell to lag behind that indicated by the ampere-hours of recharge current.

4.2 Discharging Performance of the Lead Acid Battery

The fully charged battery is allowed to discharge by keeping the AACS on, and permitted to run until the battery get fully drainage. The dynamic validation of the battery used in the test bench is shown in Figure 4. The figure shows the deterioration of the battery discharge voltage, discharge current, power consumption and the state-of-charge (SOC). Initially (the first 15 minute), when the battery is fully charged, the voltage drops (Figure 4a) across its terminal is very nominal. This zone is called exponential zone. Depending on the battery type and its health condition, this area is more or less wide. The next section represents the charge that can be extracted from the battery until the voltage drops to a certain limit. The duration of this zone is almost 70-80 minutes. Finally, the third section represents the total discharge of the battery, when the voltage drops rapidly to almost 4 volts. These similar characteristics are also observed in case of battery current and its power output. It is noted that although the battery performance is deteriorating with time, the SOC (eq. 1) is still high. Even when the battery is fully discharged at 110 minutes, the SOC is more than 60%. From eq. (1) it is observed that the battery SOC is very much dependent on the capacity $\left(C\right)$ and its initial condition. It can be noted that changing the initial condition shifts the entire SOC curve vertically.

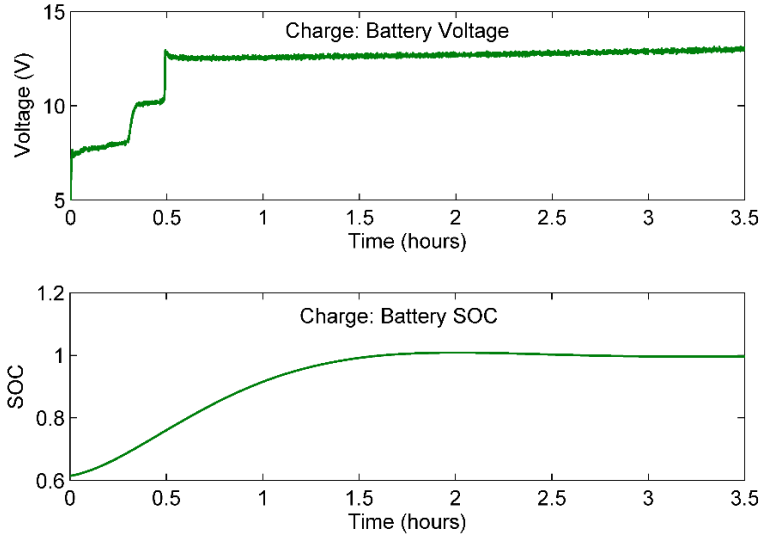

Figure 3: Charging performance of the lead-acid battery

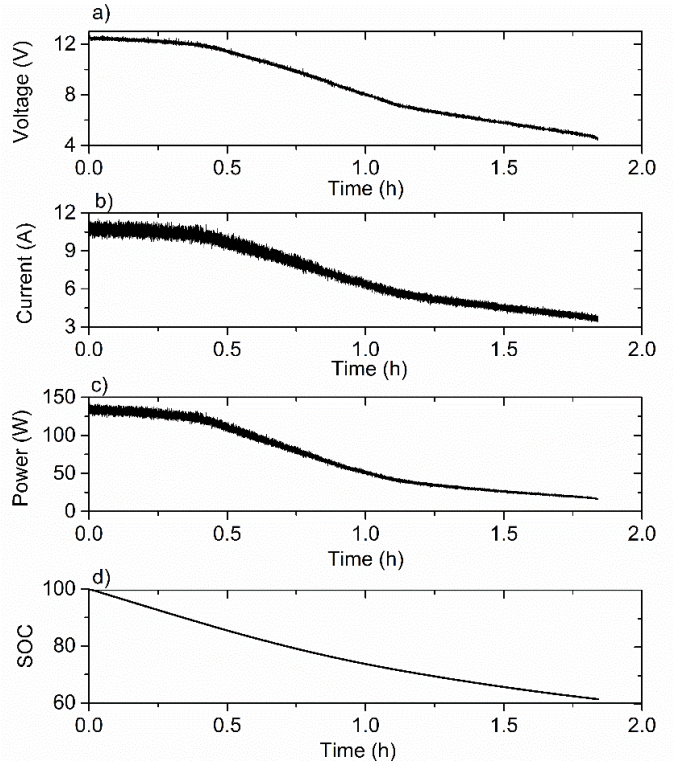

Figure 4: Discharging performance of the lead-acid battery

4.3 Effect of Battery Discharge on the Evaporator Blower and Condenser Fan Speed

As it is mentioned in section 2 that in the present test rig, the condenser fan is running in a particular speed whereas, the evaporator blower can be maintained at three different speeds by rotating a toggle switch. Figure 5 depicts the gradual decrease of the speed of the evaporator blower and the condenser fan during the discharge of the battery. From this figure it can be noted that the effect of discharge of the battery is severe in blower speed whereas, the effect is lesser in condenser fan speed.

4.4 Effect of Battery Charge on Air Velocity

Figure 6 shows the average inlet air velocity across the evaporator and the condenser surface induced by their corresponding fans at different battery terminal voltages. As the test rig does not have a facility of monitoring the air velocity continuously, the experimental results depicted in this figure have been obtained during the operation of the prime movers at the corresponding discharging voltage level of the battery. Both the air velocities across the evaporator and condenser decreases with the decrease of battery voltage. Interestingly, the rate of decrement of air velocity across the condenser surface is almost five times for the battery terminal voltage of 12 volts to 8 volts whereas, it is only two times in case of evaporator. It is obvious that with the increase of blower settings, resulting increase in blower speed has the impact to increase the air velocity across the evaporator surface.

4.5 Effect of Battery Charge on System Pressure and Temperature

Figure 7 shows the transient variation of the AACS's suction and discharge pressure with the discharging voltage of the battery. For this investigation the blower speed is set at point 3. Interestingly, the suction pressure remains constant whereas, the system discharge pressure increases with battery voltage reduction.

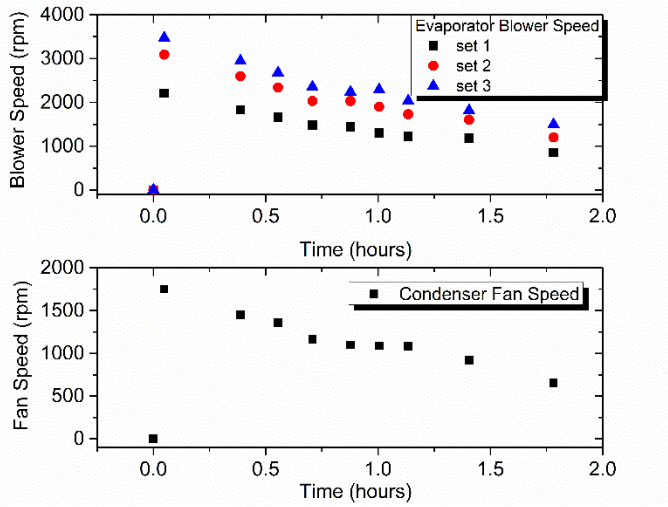

Figure 5: Fall of speed of the evaporator blower and condenser fan with battery discharge

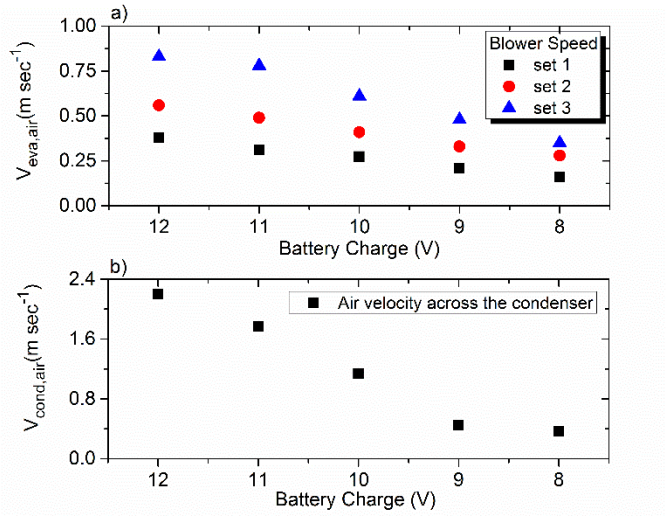

Figure 6: Variation of air velocity with battery discharging voltage

From Figure 6 it is observed that the fan speeds reduce with battery voltage drop, resulting a certain reduction in air flow rate across the heat exchangers. This variation in air flow rate reduces the evaporator outlet refrigerant temperature while, the condenser outlet refrigerant temperature increases (Figure 8). Within the range of battery terminal voltage 10 to 12 volt the variation of refrigerant temperature in both the heat exchangers are very minimum whereas, it drastically changes with further reduction of battery terminal voltage associating with enormous drop in air flow rate. At a very low air flow this may lead to frosting of the evaporator. Further, due to battery voltage drop, the fall of degree of superheat of the refrigerant, entry of wet refrigerant to the compressor cannot be ruled out.

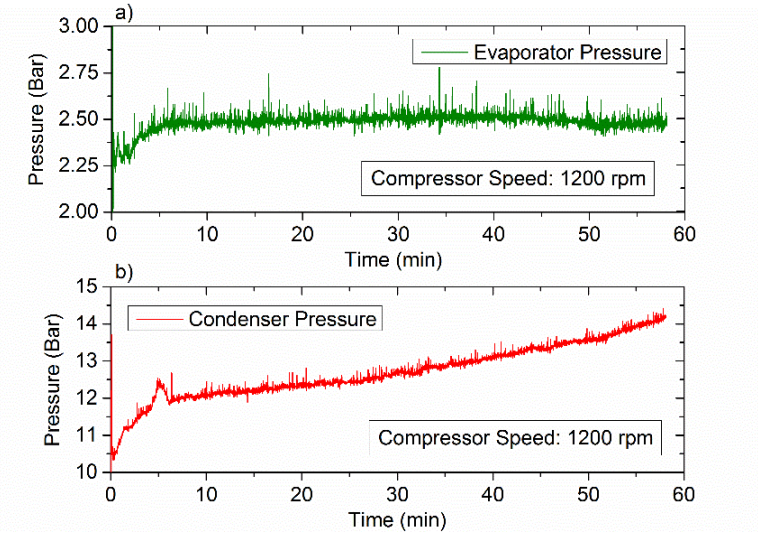

Figure 7: Variation of refrigerant suction and discharge pressure with a continuous battery voltage drop

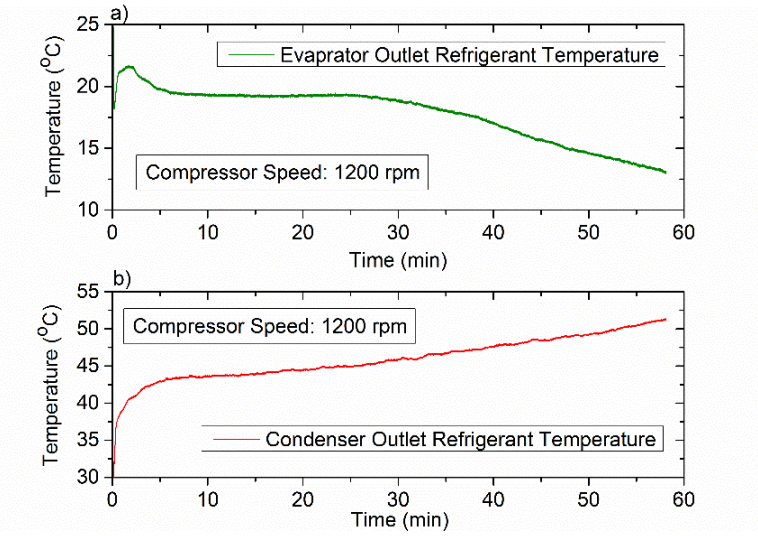

Figure 8: Variation of refrigerant suction and discharge temperature with a continuous battery voltage drop

4.6 Effect of Battery Charge on System Performance

Figure 9 shows the continuous variation of system cooling capacity, compression work, COP, and the condenser capacity with discharging of the battery. It is observed from Figure 9(a) that the system cooling capacity (eq. 3) is almost constant at the initial state of discharging. After the exponential zone of discharging (Figure 4a), it reduces marginally owing to the lack of air flow.

Opposing to the cooling capacity, the system compression work (eq. 2), which is a function of refrigerant mass flow rate and enthalpy difference, continuously increases with the reduction of battery charge (Figure 9b). From the compressor inlet and outlet pressure and temperature measurements, it is observed that the compressor inlet refrigerant enthalpy continuously decreases with the battery voltage drop whereas, the outlet enthalpy increases with the same. Finally, the increase of enthalpy gradient, resulting to the rise of system compression work with the reduction of battery charge.

Figure 9(c) shows the substantial reduction of system Coefficient of Performance (COP), which is a function of cooling capacity and compression work (eq. 5), reduces with the reduction of battery charge. It is interesting to know that the rate of increase of compression work is much more compared to the rate of reduction of cooling capacity with the battery voltage drop. As a consequence, COP is observed to fall continuously with the drop of battery voltage.

Similar to the cooling capacity, the condenser capacity (eq. 4) which is shown in Figure 9(d) is almost constant with the drop in battery terminal voltage.

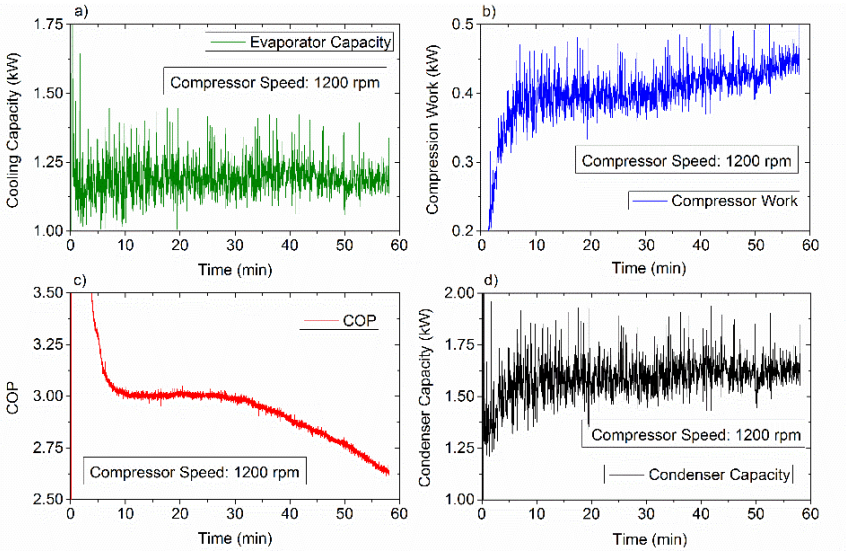

Figure 9: Variation of system cooling capacity, compression work, COP, and condenser capacity with continuous battery voltage drop

5. CONCLUSIONS

The condenser fan and the evaporator blower of an AACS receives a DC supply through a storage battery whose charge level is maintained in turn by the engine. If the supply to the battery is disrupted, the motors of the fan and the blower reduces the charge of the storage battery and thereby continuously reduce its voltage. In turn, they also run at low voltage and could only supply air at a lower flow rate. This unique dynamic condition has been investigated in detail through experimentations. Some important observations are discussed below.

- During the continuous drainage of power from the storage battery, its voltage exhibits an approximate exponential decay though its change with time is fairly linear at a low voltage value.
- As expected, the pressure and temperature of the condenser rises with the fall of air flow through it due to reduced cooling of the refrigerant.
- Though, the pressure of the evaporator does not change appreciably, there is a noticeable fall in the outlet temperature of the refrigerant through this component. This trend shows a drastic reduction in the degree of superheat. Further, at a low flow rate the exit temperature of air from the evaporator reduces. In extreme conditions this may cause frosting.
- It is fully intuitive that a reduced air flow either through the condenser or the evaporator will degrade the performance of the respective heat exchanger as well as that of the refrigeration cycle
- Operation at a decreased charge level of battery can reduce the cooling capacity by almost 35%. This is associated by an approximate increase of 30% load on the compressor. As a result, there can be a drop in COP as high as 50%.

REFERENCES

Capasso, C., & Veneri, O. (2014). Experimental analysis on the performance of lithium based batteries for road full electric and hybrid vehicles. *Applied Energy*, 1–10. http://doi.org/10.1016/j.apenergy.2014.04.013

Ceraolo, M. (2000). New dynamical models of lead–acid batteries. *IEEE Transactions on Power Systems*, *15*(4), 1184–1190.

Datta, S. P., Das, P. K., & Mukhopadhyay, S. (2013). Performance of an off-board test rig for an automotive air conditioning system. *International Journal of Air-Conditioning and Refrigeration*, *21*(3), 1350020. http://doi.org/10.1142/S201013251350020X

Datta, S. P., Das, P. K., & Mukhopadhyay, S. (2014). Effect of refrigerant charge, compressor speed and air flow through the evaporator on the performance of an automotive air conditioning system. In *15th International Refrigeration and Air Conditioning Conference at Purdue*. West Lafayette, USA.

LabVIEW. (2010). National Instruments. Retrieved from http://www.ni.com/labview

Moseley, P. T. (1997). Characteristics of a high-performance lead/acid battery for electric vehicles — an ALABC view. *Journal of Power Sources*, *67*(1-2), 115–119. http://doi.org/10.1016/S0378-7753(97)02503-2

Neubauer, J., & Wood, E. (2014). Thru-life impacts of driver aggression, climate, cabin thermal management, and battery thermal management on battery electric vehicle utility. *Journal of Power Sources*, *259*, 262–275. http://doi.org/10.1016/j.jpowsour.2014.02.083

Omar, N., Daowd, M., Hegazy, O., Al Sakka, M., Coosemans, T., Van den Bossche, P., & Van Mierlo, J. (2012). Assessment of lithium-ion capacitor for using in battery electric vehicle and hybrid electric vehicle applications. *Electrochimica Acta*, *86*, 305–315. http://doi.org/10.1016/j.electacta.2012.03.026

Veneri, O., Migliardini, F., Capasso, C., & Corbo, P. (2011). Dynamic behaviour of Li batteries in hydrogen fuel cell power trains. *Journal of Power Sources*, *196*(21), 9081–9086. http://doi.org/10.1016/j.jpowsour.2011.02.012

Xing, Y., He, W., Pecht, M., & Tsui, K. L. (2014). State of charge estimation of lithium-ion batteries using the open-circuit voltage at various ambient temperatures. *Applied Energy*, *113*, 106–115. http://doi.org/10.1016/j.apenergy.2013.07.008

Zhang, G. Y., Zhao, X. W., Qiang, J. X., Tian, F., & Yang, L. (2012). New lead-acid battery management system based on generator regulation. *International Journal of Automotive Technology*, *13*(4), 679–686. http://doi.org/10.1007/s12239−012−0066−8

ACKNOWLEDGEMENT

The authors gratefully acknowledge the financial support of General Motors India Science Lab Bangalore under the aegis of the General Motors-IIT Kharagpur Collaborative Research Laboratory.
This research work was conducted by the first author at Indian Institute of Technology Kharagpur, India during the tenure of his doctoral research.